The International Journal of Biochemistry & Cell Biology 42 (2010) 287–296

Contents lists available at ScienceDirect

The International Journal of Biochemistry & Cell Biology

journal homepage: www.elsevier.com/locate/biocel

# An adenosine derivative compound, IFC305, reverses fibrosis and alters gene expression in a pre-established $CCl_4$-induced rat cirrhosis

Julio Isael Pérez-Carreón[a,b], Lidia Martínez-Pérez[a], María Lilia Loredo[a], Lucia Yañez-Maldonado[a], Gabriela Velasco-Loyden[a], Susana Vidrio-Gómez[a], Jorge Ramírez-Salcedo[a], Francisco Hernández-Luis[c], Israel Velázquez-Martínez[c], Juan Antonio Suárez-Cuenca[a], Rolando Hernández-Muñoz[a], Victoria Chagoya de Sánchez[a,*]

[a] Departamento de Biología Celular, Instituto de Fisiología Celular, Universidad Nacional Autónoma de México (UNAM), Mexico 04510, D.F., Mexico
[b] Instituto Nacional de Medicina Genómica (INMEGEN), Periférico sur 4214, Mexico 01900, D.F., Mexico
[c] Departamento de Farmacia, Facultad de Química, Universidad Nacional Autónoma de México (UNAM), Mexico 04510, D.F., Mexico

ARTICLE INFO

*Article history:*
Received 5 August 2009
Received in revised form 19 October 2009
Accepted 6 November 2009
Available online 13 November 2009

*Keywords:*
Hepatoprotective effect
Fibrogenesis
Urea cycle
$CCl_4$ hepatotoxicity
Liver transcriptome

ABSTRACT

Cirrhosis is a complex process that involves a dynamic modification of liver cell phenotype associated to gene expression changes. This study investigates the reversing capacity of an adenosine derivative compound (IFC305) on a rat model of liver cirrhosis and gene expression changes associated with it. Rats were treated with IFC305 or saline for 5 or 10 weeks after cirrhosis induction ($CCl_4$ treatment for 10 weeks). Fibrosis score, collagenase activity and amount of hepatic stellate cells (HSC, activated and with a lipid-storing phenotype) were measured in livers. In addition, gene expression analysis was performed using 5K DNA microarrays and quantitative RT-PCR. Treatment of cirrhotic rats with IFC305 for 5 or 10 weeks compared to saline control, induced: (1) reduction of fibrosis (50–70%) and of collagen, of α-SMA and desmin proteins, as well as of activated HSCs in liver, (2) increased collagenase activity and cell number of lipid-storing HSC, (3) improved serum parameters of liver function, such as reduced activity of aminotransferases and bilirubin. Expression of 413 differential genes, deregulated in cirrhotic samples, tended to be normalized by IFC305 treatment. Some genes modulated at transcript level by IFC305 were *Tgfb1*, *Fn1*, *Col1a1*, *C9*, *Apoa1*, *Ass1*, *Cps1*, and *Pparg*. The present study shows that IFC305 reverses liver fibrosis through modulation of adipogenic and fibrosis-related genes and by ameliorating hepatic function. Thus, understanding of the anti-cirrhotic effect of IFC305 might have therapeutical potential in patients with cirrhosis.



## 1. Introduction

Cirrhosis or extensive liver fibrosis in patients is still an important cause of death worldwide. Although mortality due to cirrhosis has decreased in several countries during the last two decades, it is still extremely high in developing countries like Mexico (Bosetti et al., 2007). Cirrhosis is a highly dynamic pathological state associated to hepatic cells differentiation, phenotype changes, and cellular behavior, these events are induced by chronic liver injury that produces an inflammation process that lead to liver fibrogenesis, for review (Bataller and Brenner, 2005). Chronic damage of the liver produces hepatocyte-nodular lesions due to high cell turnover, whereas hepatic stellate cells (HSC), with a quiescent retinoid-storing phenotype, are activated to fibrogenic proliferative cell type that lack the retinoid-storing ability, these activated HSC also resemble a myofibroblast phenotype characterized by overproduction of extracellular matrix proteins (ECM), such as collagen, fibronectin, tenasin, and ondulin. Thus, parenchymal liver tissue is replaced by accumulated scar fibrous tissue, leading to deterioration of hepatic function (Friedman, 2005). Liver failure is associated, for example, with a disturbed urea cycle producing excessive blood ammonia and hepatic encephalopathy (Blei, 2004).

Chronic $CCl_4$-intoxication of rats has been extensively used as model of liver fibrosis, resulting in cirrhosis when prolonged for more than 8–12 weeks (Iredale, 2007). We reported previously the fibrosis-reversing capacity of adenosine treatment on $CCl_4$-induced cirrhotic rats. This effect has been associated with enhanced collagenolytic activity, diminution of tissue inhibitor

*Abbreviations:* ALT, alanine aminotransferase; AST, aspartate aminotransferase; α-SMA, α-smooth muscle actin; ECM, extracellular matrix proteins; HSC, hepatic stellate cell; SAH, S-adenosyl homocysteine; SAMe, S-adenosyl methionine.

* Corresponding author at: Instituto de Fisiología Celular, Universidad Nacional Autónoma de México (UNAM), Apdo. postal 70-243, México 04510, D.F., Mexico. Tel.: +52 55 5622 5614.
*E-mail address:* vchagoya@ifc.unam.mx (V.C. de Sánchez).

1357-2725/$ – see front matter © 2009 Elsevier Ltd. All rights reserved.
doi:10.1016/j.biocel.2009.11.005

of metalloproteinases (TIMPs) 1 and 2, modulation of cell redox state, maintenance of liver energy availability, and preservation of an adequate mitochondrial function of hepatic cells (Hernandez-Munoz et al., 1994, 1997, 2001). Adenosine has been proposed as a promising hepatoprotector substance for hepatic cirrhosis.

In this study, we used IFC305, an adenosine-aspartate derivative, which hypothetically includes the hepatoprotective effect of adenosine and the additional possible effect of aspartate favoring urea cycle in the liver as reported (Yassuda Filho et al., 2003). The results presented here, in $CCl_4$-model rats, demonstrate that treatment with IFC305 reversed hepatic fibrosis, reduced presence of activated HSCs, increased the number of lipid-storing HSCs, and modified global gene expression of fibrogenesis and lipid metabolism-related genes, as well as the rate-limiting enzymes of the urea cycle (Yamamoto and Sugihara, 1988). Our findings suggest that reversal of fibrosis by IFC305 could be therapeutically efficacious in the treatment of cirrhosis.

## 2. Materials and methods

### 2.1. Chemicals

$CCl_4$ was from Merck Mexico (Mexico), all other reagents were from Sigma Chemical Co. (St. Louis, MO). IFC305 is the aspartate salt of adenosine 2-aminosuccinic acid–2-(6-amino-9*H*-purin-9-yl)-5-(hydroxymethyl)tetrahydrofuran-3,4-diol (1:1). It was obtained as a white solid with the following properties; molecular Weight 400.34, melting point 285 °C, water-soluble. Synthesized by Probiomed S.A. de C.V. (http://www.probiomed.com.mx, Mexico City, Mexico).

### 2.2. Animals treatment and induction of cirrhosis with $CCl_4$

Male Wistar rats ($n = 25$) weighing 100–110 g were rendered cirrhotic by chronic treatment with $CCl_4$. Animals were intraperitoneally injected (0.4 g/kg) three times a week during 10 weeks with a solution of 1/6 of $CCl_4$ in vegetable oil. Cirrhosis-induced rats were divided in five groups (Fig. 1). At time zero (Ci-0 group), rats were euthanized 24 h after cessation of $CCl_4$, two groups were intraperitoneally treated with saline solution during 5 (Ci-5) or 10 (Ci-10) weeks and two groups were intraperitoneally treated with IFC305 at a 50 mg/kg dose, three times weekly, for 5 (Ci+A5) or 10 (Ci+A10) weeks, all the experiments include an additional group of rats without treatment (NL). Animals were euthanized with sodium pentobarbital, liver was recovered, rinsed in saline solution, and frozen with liquid nitrogen or fixed with formaldehyde, routinely processed, embedded in paraffin, and sectioned. Animals were obtained from the animal facility of the National Autonomous University of Mexico (UNAM), all procedures were conducted according to our institutional guidelines for the care and use of laboratory animals.

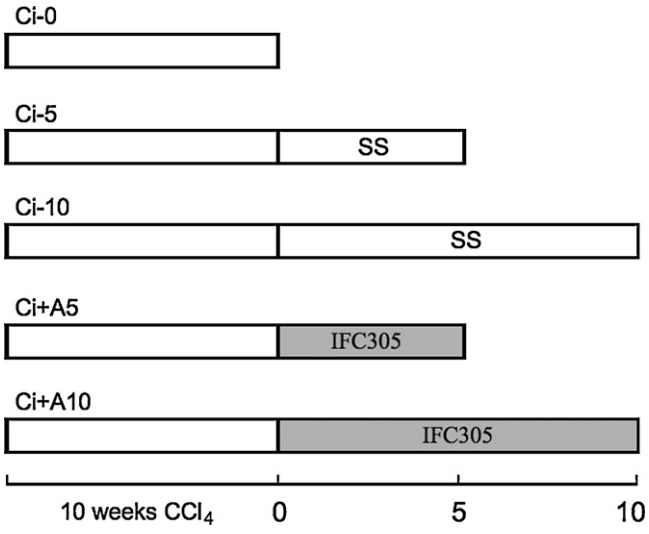


**Fig. 1.** Experimental groups to evaluate the IFC305 effect on the $CCl_4$-induced cirrhosis model. Chronic treatment of $CCl_4$ for 10 weeks induced cirrhosis. Male rats were divided in five groups; one was euthanized after $CCl_4$ withdrawal (Ci-0), while the other groups were treated with saline solution (SS) or IFC305 during 5 or 10 weeks, groups Ci-5, Ci10, Ci+A5 and Ci+A10, respectively. A group of rats without treatment (NL) was included in the experiments.

### 2.3. Fibrosis parameters measured in liver

Histological sections of liver were stained with Masson's trichrome to evaluate collagen deposition. For quantitative fibrosis data, 10 high power fields (100×) from histological sections were analyzed with the MBF_ImageJ processing software for microscopy (Abramoff et al., 2004). Blue fibrotic areas and red parenchymal tissue were detected and measured using color threshold tools in the software.

Total collagen was extracted from liver as described (Hernandez-Munoz et al., 1990). Liver homogenates were washed with ethanol and then with Tris buffer, pH 7.4, to eliminate soluble protein, collagen was extracted with 0.25 M acetic acid under continuous shaking at 4 °C for 24 h, it was hydrolyzed in 6N HCl at 110 °C for 24 h; after neutralization, its hydroxyproline content was quantified as described (Rojkind and Gonzalez, 1974). Free hydroxyproline was oxidized by chloramine-T to pyrrol, this product reacts with Ehrlich's reagent to produce a chromophore that was measured spectrophotometrically at 560 nm. Collagenase activity was determined in liver extracts, as previously described (Maruyama et al., 1982); briefly, 100 mg of protein of liver homogenates in 0.05 M Tris, 0.2 M NaCl, 5 mM $CaCl_2$ and 0.1% Triton X-100, at pH 7, was used as enzyme source and as substrate the purified collagen from rat tail, reaction was performed in 10 mM $CaCl_2$ at 37 °C for 24 h, collagen degradation products were measured by their free hydroxyproline content, as described above.

### 2.4. Serological parameters of liver function

Serum albumin, bilirubin, alanine aminotransferase (ALT), and aspartate aminotransferase (AST) activities were determined as previously described (Hernandez-Munoz et al., 1990).

### 2.5. Immunological detection of activated HSC in histological sections and liver extracts

Histological sections were used for α-smooth muscle actin (α-SMA) immunostaining, with the primary monoclonal antibody anti-α-SMA (clone 1A4 Sigma Chemical Co.) diluted at 1:200, incubating overnight (4 °C), and secondary biotinylated antibody diluted at 1:100, incubating for 1 h at room temperature, the color was revealed using the avidin–biotin complex (ABC) method. Total proteins from liver samples were separated by SDS-PAGE, transferred into nitrocellulose membranes, and incubated overnight at 4 °C with monoclonal anti-α-SMA and then with peroxidase-conjugated goat anti-mouse antibody. Alternatively membranes were incubated with goat polyclonal anti-desmin (Santa Cruz Biotechnology) and then with peroxidase-conjugated anti-goat antibody. Peroxidase activity was detected by enhanced chemiluminescence (Amersham) and quantified by densitometry using ImageJ tools.

### 2.6. Quantification of lipid-storing perisinusoidal cells in toluidine blue-stained sections

To quantify lipid-storing cells, 1-μm thick sections were obtained from samples embedded in Epon 812, and stained with toluidine blue (1% dissolved in 1% sodium tetraborate buffer; pH 9.25) as described by Hautekeete et al. (1998). The sections were examined in 10 microscopic fields at 40×, and the number of non-parenchymal cells with lipid droplets per 100 hepatocytes was counted.

### 2.7. RNA isolation and quality verification

Frozen liver samples were used for total RNA isolation by TriPure based extraction (Roche Applied Science). Quantity and purity were determined by measuring the optical density at 260/280 nm in a UV-spectrophotometer. RNA quality was verified by agarose-gel electrophoresis and rRNA 28S/18S > 1.7 ratios were obtained.

### 2.8. DNA microarray analysis

Spotted DNA microarrays were produced in our institutional DNA microarray-facility using five-thousand 70-mer oligos (Rat Array-Ready Oligo Sets vers. 1.0, Operon Biotechnologies, USA). Printing of arrays, probe preparation, hybridization, scanning of array images, and data analysis are fully detailed by Luna-Moreno et al. (2007). Briefly, 10 μg of pooled total RNA (five animals per experimental group) were used for cDNA synthesis incorporating dUTP-Cy5. Normal liver dUTP-Cy3-labeled cDNA was used as common reference. Equal quantities of Cy5- and Cy3-labeled cDNA were hybridized to the oligo rat arrays. Array images were analyzed with ArrayPro analyzer software (Media Cybernetics, Inc.). Background correction, lowest normalization and selection of differentially expressed genes were performed with GenArise software (http://www.ifc.unam.mx/genarise/). Differentially expressed genes were selected according to the *Z*-score (Cheadle et al., 2003), this function identifies differential expressed genes by calculating an intensity-dependent *Z*-score that measures the number of standard deviations (SD) from the mean (Luna-Moreno et al., 2007). Differential genes were considered up-regulated when *Z*-score > 2 SD or down-regulated if *Z*-score < −2 SD. Additionally the fold-change value (Cy5/Cy3 ratio) was computed from background-corrected and normalized Cy3 and Cy5 intensities for each element. The level of similarity of gene expression patterns was obtained by hierarchical clustering analysis, as determined by Euclidean distance and a complete linkage method using the web-available software Hierarchical Clustering Explorer (http://www.cs.umd.edu/hcil/hce/).

### 2.9. Quantitative RT-PCR

cDNA synthesis was performed from 2 μg of total RNA using SuperScript II-reverse transcriptase reagents (Invitrogen). All quantitative PCR assays were performed independently in 5 animals/group in triplicate, with standard dilution curves, using qPCR kit for SYBR Green (Sigma) on ABI prism 7000 (Applied Biosystem). PCR reactions were optimized for all genes to obtain one PCR product that corresponded to the size predicted by the primer design (Table 1). Expression data were normalized with endogenous control 18s rRNA using Taqman probe (Applied Biosystem) and presented as folds of normal liver expression.

### 2.10. Statistical analysis

Determinations were expressed as mean ± SEM of five animals as indicated in the figure footnotes. Statistically significant differences among experimental groups were determined by one-way ANOVA and the Bonferroni's multiple comparison post hoc test. Significance was set at $p < 0.05$.

## 3. Results

### 3.1. Effects of IFC305 treatment on rat cirrhosis

Accumulated liver fibrosis of $CCl_4$-treated rats associated to reduction of hepatic parenchymal tissue was clearly denoted by Masson's trichrome staining (Fig. 2A), decreased fibrosis was evident in liver of IFC305-treated animals (Fig. 2B). Quantitative analysis of histological sections shows that liver fibrosis corresponded to 16% of the area in Ci-0 group and remained at 8% at 10 weeks after $CCl_4$ withdrawal (Fig. 2C). Presence of liver fibrosis was associated to a reduced liver parenchyma area from 74% (Ci-0) to 85% at 10 weeks (Ci-10) (Fig. 2D). Treatment of cirrhotic rats with IFC305 for 5 or 10 weeks accelerated fibrosis resolution, leaving only 4% of fibrotic area, while increasing parenchyma liver area from 87 to 90%. The elevated liver collagen content (Fig. 2E) was related to reduced collagenase activity in saline-treated groups (Fig. 2F); collagen was decreased by IFC305 treatment to half-level at 5 and 10 weeks as compared to saline-treated rats, and collagenase activity was increased as clearly evidenced at 10 weeks. Reduction of fibrosis by IFC305 could be associated to increased collagenolytic activity in cirrhotic livers.

### 3.2. Recovery of liver function parameters by IFC305 treatment

Serum samples of cirrhotic rats of groups Ci-0, Ci-5 and Ci-10 displayed elevated AST, ALT and bilirubin levels, reflecting chronic hepato-biliary injury in cirrhotic rats after $CCl_4$ cessation (Table 2). Furthermore, serum albumin was relatively reduced as compared to normal control rats. IFC305 treatment for 5 weeks reduced significantly ($p < 0.05$) bilirubin and serum transaminase activities; whereas IFC305 treatment for 10 weeks significantly ($p < 0.05$) increased the serum albumin level.

### 3.3. Reduction of activated HSC by IFC305 treatment

Activation of HSC in rats can be identified with several markers such as alpha-smooth muscle actin (α-SMA), desmin and others (Van Rossen et al., 2009). Positive cells to α-SMA were detected by immunohistochemistry in hepatic fibrous septa of $CCl_4$-treated rats from 0 to 10 weeks after hepatotoxin's withdrawal (Fig. 3A).

**Table 1**
Primer sequences used in quantitative RT-PCR.

| Gene symbol | Forward (F) and reverse (R) primers |
|---|---|
| Fn1 | F: CACGGTTTCCCATTACGC<br>R: GCCATTTTCTCCCTGACG |
| Col1a1 | F: TGGATTCCAGTTCGAGTATG<br>R: AGGTGATGTTCTGGGAGGCC |
| Tgfb1 | F: AGGGCTACCATGCCAACTTCT<br>R: CCGGGTTGTGTTGGTTGTAGA |
| Pparg | F: GACATCCCGTTCACAAGAGC<br>R: GCTTTATCCCCACAGACTCG |
| Apoa1 | F: CCCAGTTTGAATCCTCCAC<br>R: CCTCGTTCCACTTCTCCTG |
| Cps1 | F: CTATTCTGAGATGTGAGATGGCTTC<br>R: AGCGCTGTACTGCCTGTAGTGGAA |
| Ass1 | F: CCAGGAAGAAGGCACTGAAG<br>R: CGCCGTGAGACACATACTTG |
| C9 | F: GTCAAAACGGAGGCACAG<br>R: CTTGGCAGTGAGGATTCG |

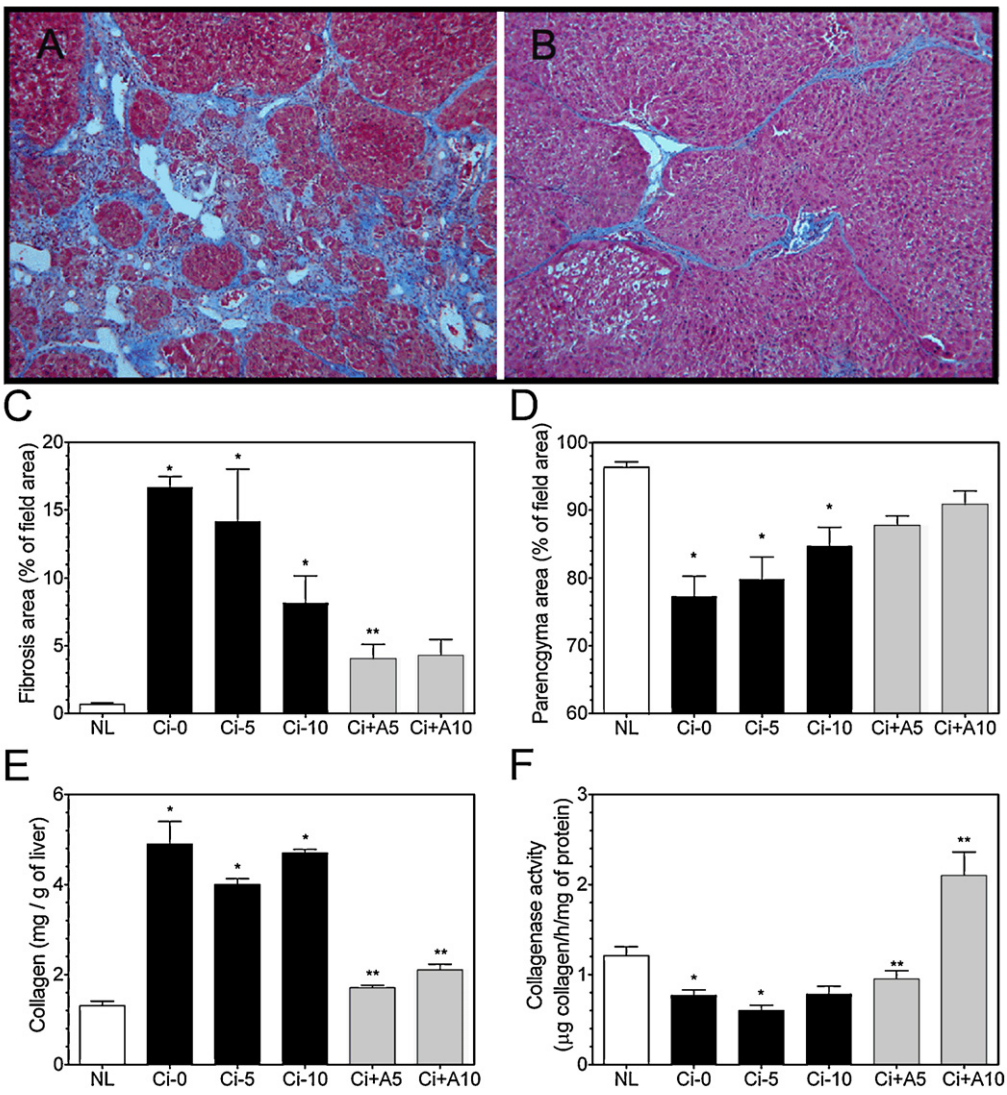


**Fig. 2.** IFC305 reduces fibrosis and collagen in cirrhotic livers. Masson's trichromic stained histological section revealed marked fibrosis in cirrhotic livers Ci-5 (A) and moderate fibrosis in rats treated with IFC305 for 5 weeks Ci+A5 (B). Quantitative image analysis of fibrosis blue areas (C) and parenchyma red areas (D). Amount of total collagen (E) and collagenase activity (F) in liver extracts. Data represent mean ± SEM of 5 rats/group. *Statistical difference ($p < 0.01$) compared to NL group. **Statistical difference ($p < 0.01$) when compared to their respective experimental group Ci-5 or Ci-10. (For interpretation of the references to color in this figure legend, the reader is referred to the web version of the article.)

IFC305 treatment reduced the presence of α-SMA-positive cells by 50% when compared to saline-treated cirrhotic rats (Fig. 3B and C). Similarly, as assessed through western blot analysis, this treatment reduced abundance of α-SMA and desmin proteins in liver extracts when compared to $CCl_4$-cirrhotic rats (Fig. 3D). This reduction corresponded to more than 50% when compared with groups at 5 or 10 weeks.

**Table 2**
Serological parameters of liver function.

| Group | Albumin[a] | Bilirubin[b] | ALT[c] | AST[c] |
|---|---|---|---|---|
| Control | 3.5 ± 0.098 | 0.8 ± 0.063 | 42 ± 1.558 | 179 ± 5.369 |
| Ci-0 | 2.2 ± 0.039* | 2.3 ± 0.271* | 324 ± 14.318* | 396 ± 33.544* |
| Ci-5 | 3.1 ± 0.189 | 2.1 ± 0.210* | 300 ± 13.045* | 389 ± 29.646* |
| Ci-10 | 2.5 ± 0.061* | 1.4 ± 0.144* | 145 ± 11.316* | 229 ± 15.707 |
| Ci+A5 | 3.6 ± 0.119 | 1.0 ± 0.046** | 81 ± 9.295** | 215 ± 14.555** |
| Ci+A10 | 3.1 ± 0.065** | 1.1 ± 0.127 | 119 ± 8.717 | 237 ± 16.569 |

Mean ± SEM of 5 animals/group.
Alanine aminotransferase (ALT) and aspartate aminotransferase (AST).
[a] g/dL.
[b] mg/dL.
[c] U/dL.
* Statistical difference compared to control group.
** Statistical difference compared to Ci-5 or Ci-10 group.

### 3.4. Restored presence of lipid-storing HSC by IFC305 treatment in cirrhotic rats

Morphological analyses of histological sections of a normal liver stained with toluidine blue revealed typical HSC in a quiescent state with abundant lipid droplets in their cytoplasm, the number of HSCs detected was 6 per 100 hepatocytes (Fig. 4A and D). A significant decrease (less than 1 cell/250 hepatocytes) of lipid-storing HSCs was detected in Ci-0 and Ci-5 groups of cirrhotic rats (Fig. 4B and D); IFC305 treatment during 5 weeks almost restored the presence of HSCs (5 cells/100 hepatocytes) with more than four lipid droplets per cell (Fig. 4C and D).

### 3.5. Effect of IFC305 on global gene expression profiles in cirrhotic livers

Total RNA from liver of experimental groups was obtained for DNA microarrays analysis to study gene expression patterns associ-

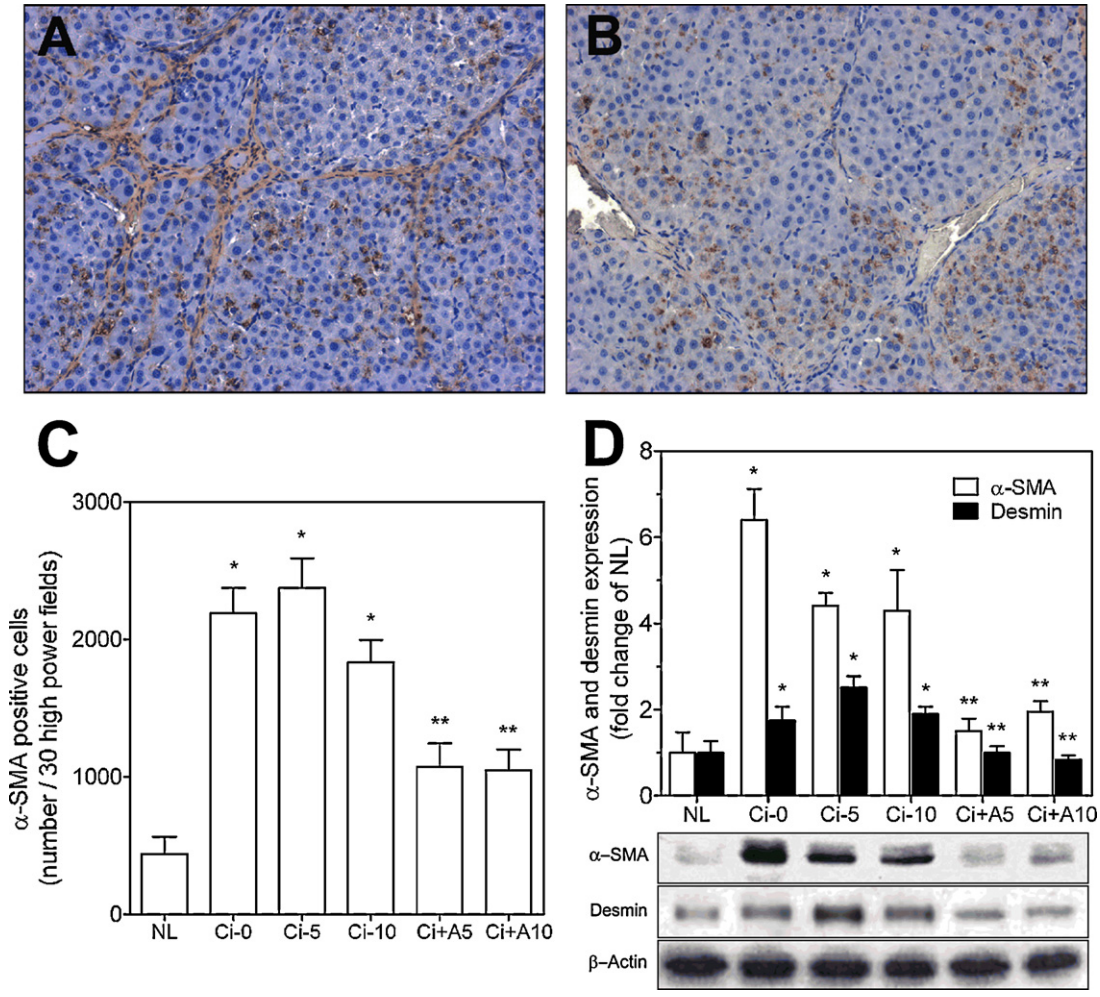


**Fig. 3.** Effect of IFC305 on the presence of and activated HSCs in the cirrhotic liver. Immunohistochemical staining of α-SMA-positive cells in fibrous septa of a rat of group Ci-5 (A) and from a rat treated with IFC305 Ci-A5 (B). Quantitative image analysis of α-SMA-positive cells (C). Protein level of α-SMA and desmin in liver extracts (D); representative western blot images are shown at the bottom and the densitometric analysis in the upper part. β-Actin immunodetection was used as a loading control. Data represent mean ± SEM from 5 rats/group. *Statistical difference ($p < 0.05$) compared to NL group. **Statistical difference ($p < 0.05$) when compared to their respective experimental group Ci-5 or Ci-10.

ated to the effect of IFC305 in cirrhotic rats. The two-color (Cy5/Cy3) microarray experiment was designed to hybridize samples from each group against a common reference, a pool of RNA from livers of five untreated rats. Differentially expressed genes were selected from cirrhotic groups (Ci-0, Ci-5 and Ci-10) by the *Z*-score method (Luna-Moreno et al., 2007) and compared to the IFC305-treatment groups (Ci+A5 and Ci+A10). The detailed list of 413 selected genes is given in the Supplementary Table A and projected as a hierarchical clustering in Fig. 5A. Differential genes were grouped by their similarities at transcript level, as up-regulated (red) or down-regulated (green). Based on their molecular function, the highest proportion was classified as signal transduction genes (Supplementary Figure A). From selected genes, those genes involved in TGF-β signaling pathway, lipid metabolism, urea cycle, and fibrogenesis were identified and highlighted in Fig. 5A. When gene expression profile was compared by two-dimensional hierarchical clustering (genes and experimental groups) and similarity of groups was represented in a dendrogram (Fig. 5B), the highest similarity pattern corresponded to both IFC305 treatments at 5 and 10 weeks, whereas the highest difference was found between Ci+A5 and Ci-5 groups implying that the IFC305 treatment was able to modify the gene expression pattern of cirrhotic livers. Graphs in Fig. 5C further reveal that global expression of both, up-regulated genes (upper panel) and down-regulated genes (lower panel), in cirrhotic livers (Ci-5 and Ci-10), is modified by IFC305 treatment with a clear tendency towards the normal liver expression (ratio of 1).

### 3.6. *Effect of IFC305 on gene expression as analyzed by qRT-PCR*

The IFC305 effect on some genes involved in liver fibrosis and cirrhosis was determined through qRT-PCR using SYBR Green method and specific primers (Table 1). Transcript level of the fibrogenesis-related genes *Fn1* and *Col1a1* was higher in cirrhotic than in normal livers, and IFC305 treatment reduced gene expression to a normal level (Fig. 6). Expression of these two genes is modulated by the TGF-β signaling pathway and some of these related genes were modulated at the transcript level as shown by DNA microarray analysis (Fig. 5A, black gene symbols), the expression of *Tgfb1* was increased markedly in cirrhotic rats of Ci-0 and Ci-5 groups, and treatment of IFC305 during 5 weeks reduced this transcript level to the normal value (Fig. 6). Significant differences of gene expression between saline and IFC305-treated rats at 5 weeks were found; for example, the high expression of complement *C9* and *Apoa1* genes in cirrhotic livers was reduced by IFC305 treatment. The peroxisome proliferator-activated receptor gamma (PPARγ) regulates cellular fatty acid storage, adipogenesis of fibroblasts and there are interesting findings that support the role of this receptor in reversion of activated HSCs toward quiescent HSCs

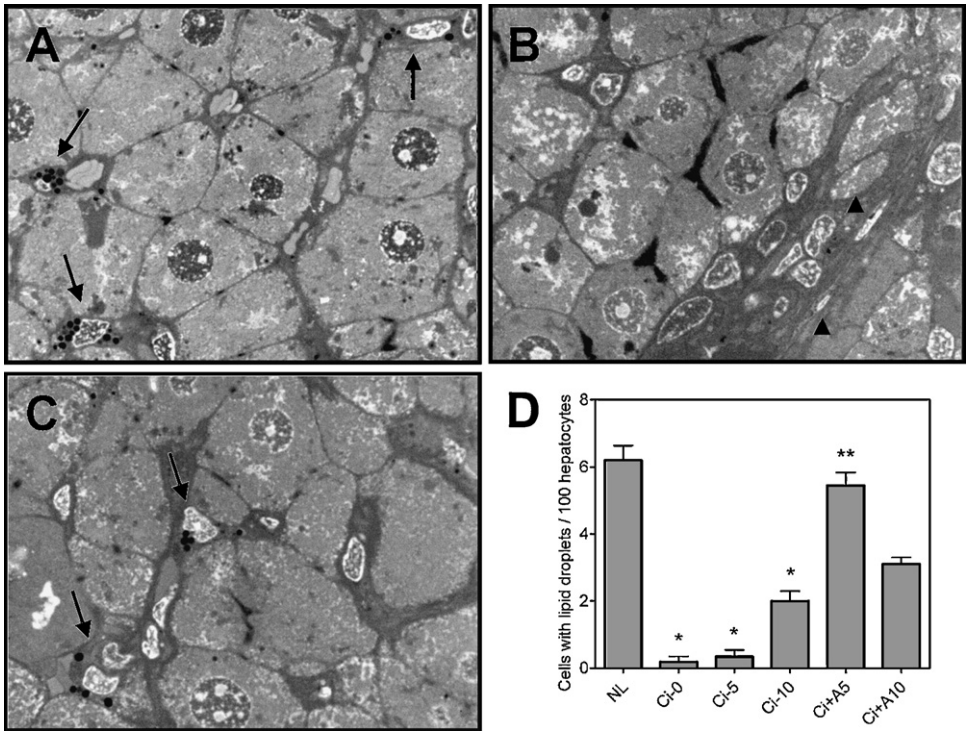


**Fig. 4.** Effect of IFC305 on the presence of HSC with lipid droplets in the cirrhotic liver. Liver thin histological sections stained with toluidine blue to denote lipid-storing HSCs (arrows) from a normal rat (A), a rat of group Ci-5 activated HSCs (head arrow) (B), and a rat of group Ci+A5 (C). Number of non-parenchymal cells with lipid droplets were counted and normalized by the number of hepatocytes in a microscope with a 40× objective. (D) Data represent mean ± SEM from 5 rats/group. *Statistical difference ($p < 0.05$) compared to NL group. **Statistical difference ($p < 0.05$) when compared to their respective experimental group Ci-5 or Ci-10.

(Hazra et al., 2004a). Congruently with reports that shows declined expression of its gene *Pparg* in liver fibrosis (de Gottardi et al., 2006; Yang et al., 2006), we found a low transcript level of *Pparg* in cirrhotic livers; Ci-0 and Ci-10 groups revealed a significant statistical difference when compared to normal liver values; whereas IFC305 treatment restored *Pparg* levels to values similar to those of the normal liver. DNA microarray analysis revealed three genes involved in ornithine and urea metabolism (Fig. 5A, green gene symbols), the transcript level of *Ass1* was reduced to 30–40% of that of the normal liver, whereas, in Ci+A5 and Ci+A10 groups, a partial recovery to 60–80% of normal liver expression level was observed. Similarly, *Cps1* expression was reduced in the Ci-5 group and restored to normal level in the Ci+A5 group, even the Ci+A10 group showed increased *Cps1* transcript level over normal expression. Thus, through this quantitative analysis of mRNA abundance, the IFC305 shows capabilities to modulate gene expression of some important genes involved in liver fibrogenesis.

## 4. Discussion

This *in vivo* study was designed to analyze the effect of an adenosine derivative compound, IFC305, on the reversibility of $CCl_4$-induced liver cirrhosis in rats. Fibrogenic events, such as increased collagen deposition, decreased number of quiescent HSCs and increased presence of fibroblastic α-SMA-positive cells persisted in cirrhotic samples at 5 and 10 weeks after $CCl_4$ cessation. Parameters indicative of liver dysfunction (AST, ALT, and bilirubin) were increased in rat sera. Other indicators of liver damage were reduction of hepatic parenchyma, reduction of liver collagenase activity, and low albumin serum levels. Particularly, the IFC305 treatment was able to reverse several fibrosis markers, including amelioration of serological parameters of liver function. Furthermore, some differential genes deregulated in cirrhotic samples identified by DNA microarray were modulated by IFC305 treatment with tendencies to normal expression (Fig. 5).

We have previously studied the fibrogenic reversing capacity of adenosine on rat livers (Hernandez-Munoz et al., 1994, 1997, 2001) and, as shown in the present study, the adenosine derivative, IFC305, possesses similar hepatoprotective capacities towards reducing fibrosis. Considering previous findings of adenosine effects on experimental cirrhosis, we infer that IFC305 effects may be attributed to its adenosine constituent. Adenosine is a purine nucleoside that acts as chemical messenger with autocrine, paracrine, and endocrine actions (Chagoya de Sanchez, 1995). The multiphysiological action of adenosine could be mediated through diverse biochemical events, cell signaling mediated by adenosine receptors (A1, A2a, A2b, and A3), energy homeostasis of the cell involving phosphotransfer reactions of adenine nucleotides, as well as through the methionine-homocysteine cycle that is important for methyl group transfer reactions such as DNA methylation. Under physiological conditions, adenosine is mainly formed by two metabolic sources, the phosphohydrolysis of adenine nucleotides and the hydrolysis of S-adenosyl homocysteine formed by the demethylation of S-adenosyl methionine (SAMe). Reduced levels of adenine nucleotides and SAMe have been detected in patients with liver damage, including cirrhosis (Duce et al., 1988; Hernandez-Munoz et al., 1991; Martinez-Chantar et al., 2002). Rats liver of $CCl_4$-induced cirrhosis, similarly to liver of human cirrhotic patients, showed that metabolic sources of adenosine are impaired as a result of the diminution of adenine nucleotides, the loss of energy status and redox equilibrium of cells. Evidence with adenosine treatment, which restituted these metabolic routes, indicates its hepatoprotective actions (Chagoya de Sanchez et al., 1995; Hernandez-Munoz and Chagoya de Sanchez, 1994; Hernandez-Munoz et al., 1992, 1994, 1997). Some results obtained by dietary supplementation of adenosine-related metabolites such

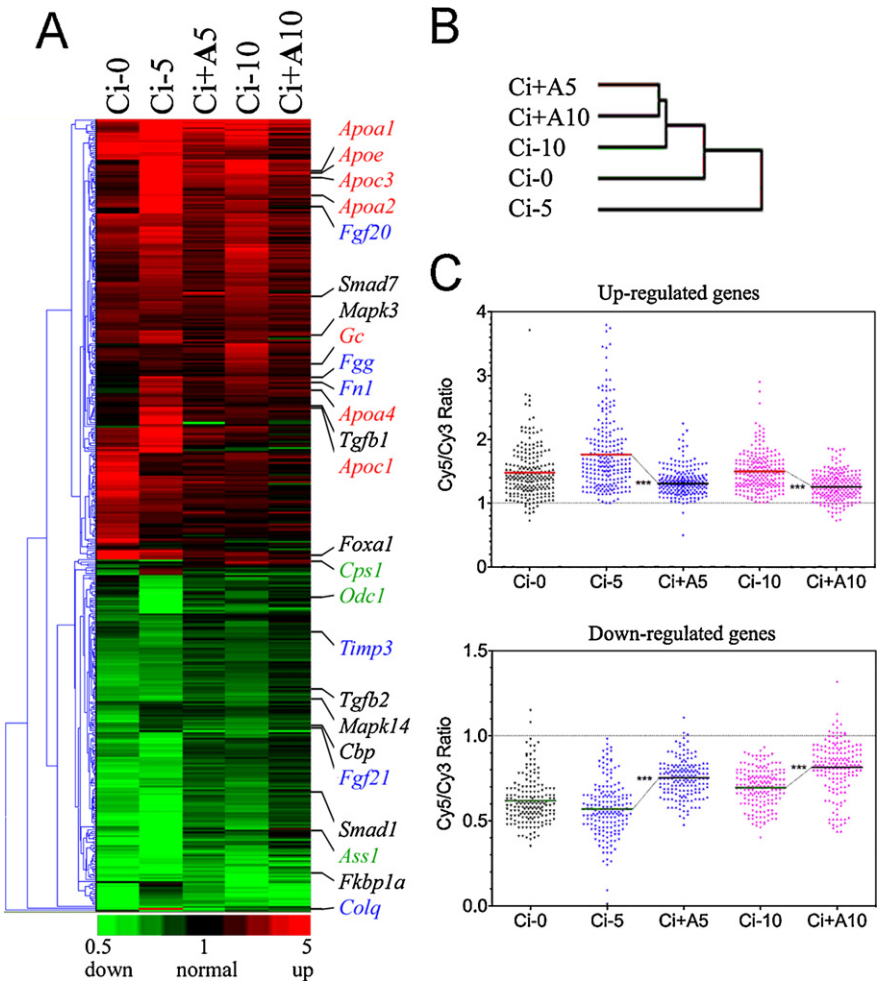


**Fig. 5.** Effect of IFC305 treatment on global gene expression profile in cirrhotic livers. (A) Hierarchical clustering of 413 differential genes (Selected by *Z*-score value) comparing experimental treatments. Color value indicates the normalized Cy5/Cy3 ratio compared with normal liver NL (ratio 1). Symbol of genes involved in lipid metabolism (red), fibrogenesis (blue), urea cycle (green), and TGF-β signaling (black) are indicated on the right side. (B) Unsupervised hierarchical clustering denotes differential profile signatures between Ci-A and Ci groups at both times (5 and 10 weeks). (C) Plots of up-regulated (upper panel) and down-regulated genes (lower panel) denote that average expression tends to normal expression in Ci-A groups when compared to Ci groups. ***Statistical difference ($p < 0.001$) in groups indicated with a diagonal line (mean difference). (For interpretation of the references to color in this figure legend, the reader is referred to the web version of the article.)

as nucleotides (Carver, 1994; Perez et al., 2004) and SAMe administration (Karaa et al., 2008; Marchesini et al., 1992) showed hepatoprotective action, and are in agreement with this potential action of adenosine on liver damage induced in animal models.

During fibrogenesis, activated HSC phenotype is characterized by loss of lipid droplets containing retinoids, high expression of ECM components, and elevated expression of intermediate filaments, such as α-SMA and desmin. IFC305 was able to reduce α-SMA-positive cells and the abundance of α-SMA and desmin proteins in liver extracts increased also the number of lipid-storing HSCs in cirrhotic livers (Figs. 3 and 4); the proposed mechanistic possibilities for this result are induction of myofibroblastic cells apoptosis, inhibition of HSCs activation and their proliferative capacity, and re-differentiation of myofibroblastic cells to an α-SMA-negative phenotype. Several substances, such as curcumin, selenium, tetrandine and an Hsp90-inhibitor have shown hepatoprotective effects in vivo through different molecular mechanisms of action, just as the induction of apoptosis in HSC or delaying their activation (Ding et al., 2009; Myung et al., 2009; Priya and Sudhakaran, 2008; Yin et al., 2007).

Recent reviews point out the importance of the diminution of PPARγ in HSCs activation during experimental and human cirrhosis, as well as its re-expression for the reversal of pro-fibrogenic phenotype (Atzori et al., 2009; Mann and Mann, 2009). PPARγ is a member of the nuclear-receptor superfamily that transcriptionally regulates adipogenic cellular phenotype, proliferation, lipid uptake and storage. Its activation is ligand-dependent, agonists, such as thiazolidinediones, have been proposed to induce PPARγ dependent responses in the liver (Marra and Pastacaldi, 2002); for example, treatment with rosiglitazone resulted in inhibition of experimental-induced cirrhosis through reduction of HSC proliferation (Bruck et al., 2009). Increased expression of PPARγ (vector-mediated expression or induced by its ligand 15dPGJ2) in activated HSCs reverses their phenotype to a quiescent state with accumulation of retinoids, reduced stress fibers, and prominent dendritic processes (Hazra et al., 2004a,b). It is notable that the reduced transcript level of *Pparg* in cirrhotic livers in our model is being re-established by IFC305 treatment, indicating a probable prevention of HSCs activation and/or a reversion of activated HSCs to a quiescent state with accumulation of lipid droplets.

Confirming the potential of this adenosine compound to revert cirrhosis, both up- and down-regulated genes in cirrhotic groups tended to be normalized with IFC305 treatment. As expected, high transcript levels of the profibrotic cytokine, *Tgfb1*, and two ECM genes, *fibronectin 1* (*Fn1*) and *collagen type 1 alpha 1* (*Col1a1*) were detected in cirrhotic livers (Fig. 6). Increased expression of ECM genes in fibrotic livers could be induced by activated HSCs (Ramadori et al., 1992; Stefanovic et al., 1997), and the main fibro-

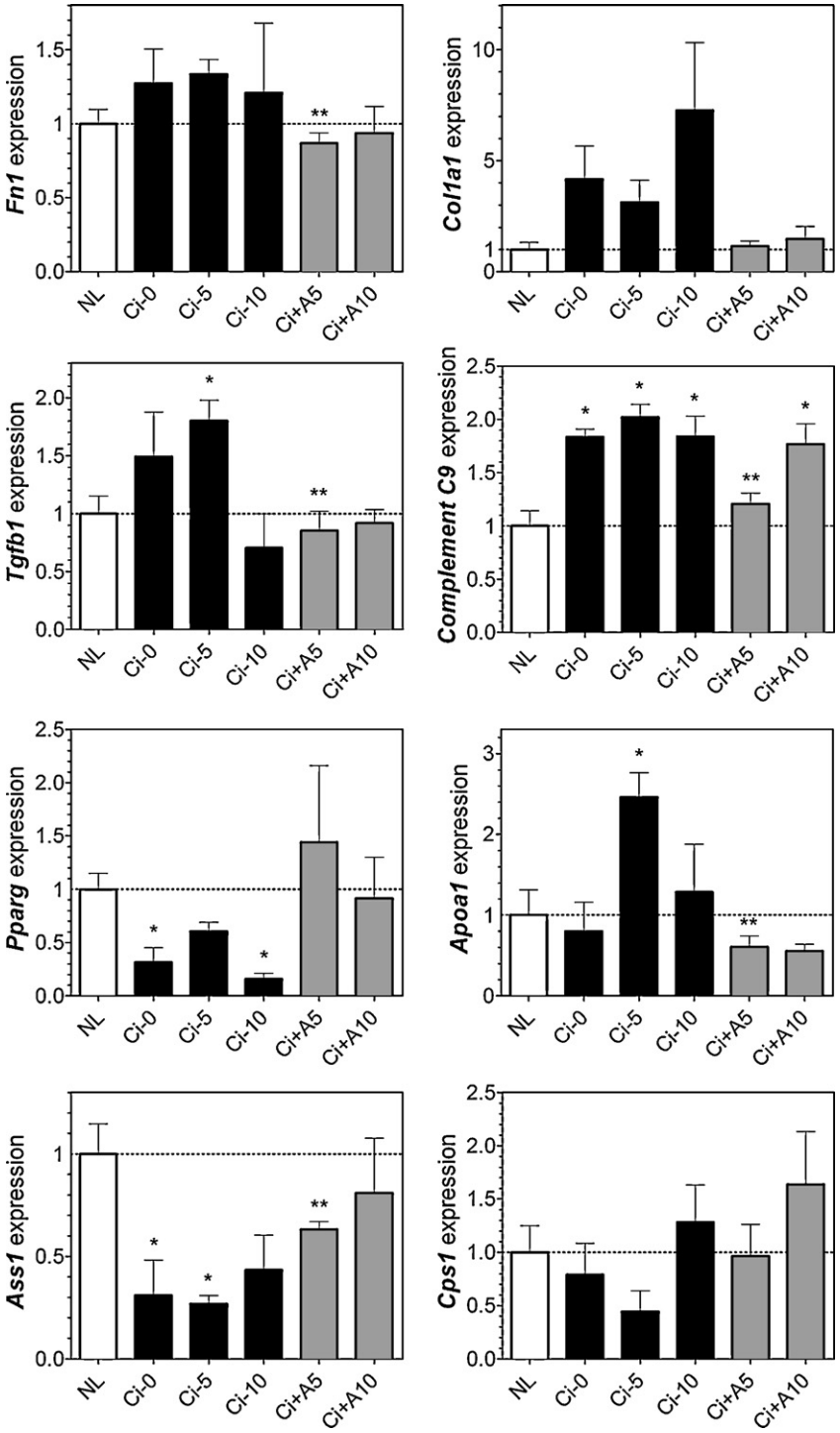


**Fig. 6.** Effect of IFC305 treatment on expression of eight genes in cirrhotic livers measured by quantitative RT-PCR. The mRNA level of *Fn1*, *Col1a1*, *Tgfb1*, *C9*, *Pparg*, *Apoa1*, *Ass1* and *Cps1* was measured and referred to normal liver (NL) level. Arbitrary expression values were normalized to eukaryotic 18S rRNA control gene level. Data represent mean ± SEM from 5 rats/group. *Statistical difference ($p < 0.05$) compared to NL group. **Statistical difference ($p < 0.05$) when compared to their respective experimental group Ci-5 or Ci-10.

genic mediator is TGF-β (Knittel et al., 1996). IFC305 treatment reduced expression of these genes, supporting the idea that HSCs activation is one cellular target of this compound. Furthermore a set of nine differential genes related to TGF-β signaling (*Tgfb1*, *Smad7*, *Fkbp1a*, *Hnf3a*, *Tgfb2*, *Mapk3*, *Cbp*, *Smad1*, *Mapk14*) was identified by DNA microarray analysis; this pathway plays a central role in a number of developmental and pathological processes including liver fibrosis (Verrecchia and Mauviel, 2007). TGF-β activates HSCs through two intracellular signaling downstream of the TGF-β receptors: the Smad and the p38 (*Mapk14*) signaling; both pathways are independently involved in collagen (*Col1a1*) gene expression (Parsons et al., 2007; Tsukada et al., 2005). Although changes in gene expression, such as the TGF-β signaling in cirrhotic livers could be associated to activation of HSCs, it must be considered that the resultant gene expression in the fibrotic liver comes from different hepatic and inflammatory cells. Nonetheless, IFC305 had the ability to reduce the high *Tgfb1 expression* in the whole tissue.

Other genes with increased expression in cirrhotic rats were apolipoprotein genes (*Apoa1*, *Apoa2*, *Apoa4*, *Apoc1*, *Apoc3*, *Apoe*), which could be the result of a disturbed lipid metabolism in the liver. Increased mRNA level of *Apoa1* has been associated with liver steatosis in humans (Mathurin et al., 1996). Transcriptional regulation of human apolipoproteins AI, AIV, and CIII has been determined to be stimulated by the TGF-β cytokine through Smad 3/4 signaling (Zannis et al., 2001). Thus, decreased mRNA levels of apolipoprotein genes in the IFC305-treated groups could be due to decreased expression of the *Tgfb1* gene.

One of the major complications of patients with cirrhosis is hepatic encephalopathy characterized by increased blood ammonia level (Mesejo et al., 2008). Ammonia detoxification mainly occurs in the liver through the urea cycle and the two main rate-limiting enzymes of this cycle are argininosuccinate synthetase 1 (Ass1) (Husson et al., 2003) and carbamoyl-phosphate synthetase 1 (Cps1). We found that cirrhotic rats presented lower transcript levels of *Ass1* and *Cps1* than normal rats and high blood level of ammonia has been measured in the $CCl_4$-induced cirrhosis model (Yamamoto and Sugihara, 1987). Considering that IFC305 treatment restored partially their hepatic expression (Figs. 5 and 6) its use for the treatment of patient with cirrhosis and hepatic encephalopathy could be promising.

In conclusion, this study provides support that IFC305 treatment reversed liver fibrosis and ameliorated hepatic function in the $CCl_4$-induced cirrhotic rats. The IFC305 reversing effect could be associated to a modulation of fibrosis-related genes at the mRNA level, restoring their normal expression, possibly avoiding activation of HSCs and inducing re-differentiation of the activated HSCs. Thus, fully understanding and exploring the IFC305's anti-cirrhotic effect could lead to a considerable clinical potential in patients with chronic liver diseases.

## Acknowledgments

We thank S. Guzmán, J. Santillán and L. Chávez from our institutional Microarray facility, G. Coello, G. Corral and A. Gómez for GenArise software assistance. R. Paredes for microscopy studies, and J. Barbosa for image design. Grant support from Consejo Nacional de Ciencia y Tecnología CONACYT 41433-Q

## Appendix A. Supplementary data

Supplementary data associated with this article can be found, in the online version, at doi:10.1016/j.biocel.2009.11.005.

## References

Abramoff MD, Magelhaes PJ, Ram SJ. Image processing with image. J Biophoton Int 2004;11:36–42.
Atzori L, Poli G, Perra A. Hepatic stellate cell: a star cell in the liver. Int J Biochem Cell Biol 2009;41:1639–42.
Bataller R, Brenner DA. Liver fibrosis. J Clin Invest 2005;115:209–18.
Blei AT. Infection, inflammation and hepatic encephalopathy, synergism redefined. J Hepatol 2004;40:327–30.
Bosetti C, Levi F, Lucchini F, Zatonski WA, Negri E, La Vecchia C. Worldwide mortality from cirrhosis: an update to 2002. J Hepatol 2007;46:827–39.
Bruck R, Weiss S, Aeed H, Pines M, Halpern Z, Zvibel I. Additive inhibitory effect of experimentally induced hepatic cirrhosis by agonists of peroxisome proliferator activator receptor gamma and retinoic acid receptor. Dig Dis Sci 2009;54:292–9.
Carver JD. Dietary nucleotides: cellular immune, intestinal and hepatic system effects. J Nutr 1994;124:144S–8S.
Chagoya de Sanchez V. Circadian variations of adenosine and of its metabolism. Could adenosine be a molecular oscillator for circadian rhythms? Can J Physiol Pharmacol 1995;73:339–55.
Chagoya de Sanchez V, Hernandez-Munoz R, Yanez L, Vidrio S, Diaz-Munoz M. Possible mechanism of adenosine protection in carbon tetrachloride acute hepatotoxicity. Role of adenosine by-products and glutathione peroxidase. J Biochem Toxicol 1995;10:41–50.
Cheadle C, Vawter MP, Freed WJ, Becker KG. Analysis of microarray data using Z score transformation. J Mol Diagn 2003;5:73–81.
de Gottardi A, Pazienza V, Pugnale P, Bruttin F, Rubbia-Brandt L, Juge-Aubry CE, et al. Peroxisome proliferator-activated receptor-alpha and -gamma mRNA levels are reduced in chronic hepatitis C with steatosis and genotype 3 infection. Aliment Pharmacol Ther 2006;23:107–14.
Ding M, Potter JJ, Liu X, Torbenson MS, Mezey E. Selenium supplementation decreases hepatic fibrosis in mice after chronic carbon tetrachloride administration. Biol Trace Elem Res 2009.
Duce AM, Ortiz P, Cabrero C, Mato JM. S-adenosyl-L-methionine synthetase and phospholipid methyltransferase are inhibited in human cirrhosis. Hepatology 1988;8:65–8.
Friedman SL. Mac the knife? Macrophages—the double-edged sword of hepatic fibrosis. J Clin Invest 2005;115:29–32.
Hautekeete ML, Dodeman I, Azais-Braesco V, Van den Berg K, Seynaeve C, Geerts A. Hepatic stellate cells and liver retinoid content in alcoholic liver disease in humans. Alcohol Clin Exp Res 1998;22:494–500.
Hazra S, Miyahara T, Rippe RA, Tsukamoto H. PPAR gamma and hepatic stellate cells. Comp Hepatol 2004a;3(Suppl. 1):S7.
Hazra S, Xiong S, Wang J, Rippe RA, Krishna V, Chatterjee K, et al. Peroxisome proliferator-activated receptor gamma induces a phenotypic switch from activated to quiescent hepatic stellate cells. J Biol Chem 2004b;279:11392–401.
Hernandez-Munoz R, Chagoya de Sanchez V. In vivo correlation between liver and blood energy status as evidenced by chronic treatment of carbon tetrachloride and adenosine to rats. Can J Physiol Pharmacol 1994;72:1252–6.
Hernandez-Munoz R, Diaz-Munoz M, Chagoya de Sanchez V. Effects of adenosine administration on the function and membrane composition of liver mitochondria in carbon tetrachloride-induced cirrhosis. Arch Biochem Biophys 1992;294:160–7.
Hernandez-Munoz R, Diaz-Munoz M, Chagoya de Sanchez V. Possible role of cell redox state on collagen metabolism in carbon tetrachloride-induced cirrhosis as evidenced by adenosine administration to rats. Biochim Biophys Acta 1994;1200:93–9.
Hernandez-Munoz R, Diaz-Munoz M, Lopez V, Lopez-Barrera F, Yanez L, Vidrio S, et al. Balance between oxidative damage and proliferative potential in an experimental rat model of CCl4-induced cirrhosis: protective role of adenosine administration. Hepatology 1997;26:1100–10.
Hernandez-Munoz R, Diaz-Munoz M, Suarez J, Chagoya de Sanchez V. Adenosine partially prevents cirrhosis induced by carbon tetrachloride in rats. Hepatology 1990;12:242–8.
Hernandez-Munoz R, Diaz-Munoz M, Suarez-Cuenca JA, Trejo-Solis C, Lopez V, Sanchez-Sevilla L, et al. Adenosine reverses a preestablished CCl4-induced micronodular cirrhosis through enhancing collagenolytic activity and stimulating hepatocyte cell proliferation in rats. Hepatology 2001;34:677–87.
Hernandez-Munoz R, Glender W, Diaz-Munoz M, Suarez J, Lozano J, Chagoya de Sanchez V. Alterations of ATP levels and of energy parameters in the blood of alcoholic and nonalcoholic patients with liver damage. Alcohol Clin Exp Res 1991;15:500–3.
Husson A, Brasse-Lagnel C, Fairand A, Renouf S, Lavoinne A. Argininosuccinate synthetase from the urea cycle to the citrulline-NO cycle. Eur J Biochem 2003;270:1887–99.
Iredale JP. Models of liver fibrosis: exploring the dynamic nature of inflammation and repair in a solid organ. J Clin Invest 2007;117:539–48.
Karaa A, Thompson KJ, McKillop IH, Clemens MG, Schrum LW. S-adenosyl-L-methionine attenuates oxidative stress and hepatic stellate cell activation in an ethanol-LPS-induced fibrotic rat model. Shock 2008;30:197–205.
Knittel T, Janneck T, Muller L, Fellmer P, Ramadori G. Transforming growth factor beta 1-regulated gene expression of Ito cells. Hepatology 1996;24:352–60.
Luna-Moreno D, Vazquez-Martinez O, Baez-Ruiz A, Ramirez J, Diaz-Munoz M. Food restricted schedules promote differential lipoperoxidative activity in rat hepatic subcellular fractions. Comp Biochem Physiol A Mol Integr Physiol 2007;146:632–43.
Mann J, Mann DA. Transcriptional regulation of hepatic stellate cells. Adv Drug Deliv Rev 2009;61:497–512.
Marchesini G, Bugianesi E, Bianchi G, Fabbri A, Marchi E, Zoli M, et al. Effect of S-adenosyl-L-methionine administration on plasma levels of sulphur-containing amino acids in patients with liver cirrhosis. Clin Nutr 1992;11:303–8.
Marra F, Pastacaldi S. Thiazolidinediones and PPARgamma system in repair of liver damage. Recenti Prog Med 2002;93:9–15.
Martinez-Chantar ML, Garcia-Trevijano ER, Latasa MU, Perez-Mato I, Sanchez del Pino MM, Corrales FJ, et al. Importance of a deficiency in S-adenosyl-L-methionine synthesis in the pathogenesis of liver injury. Am J Clin Nutr 2002;76:1177S–82S.
Maruyama K, Feinman L, Fainsilber Z, Nakano M, Okazaki I, Lieber CS. Mammalian collagenase increases in early alcoholic liver disease and decreases with cirrhosis. Life Sci 1982;30:1379–84.
Mathurin P, Vidaud D, Vidaud M, Bedossa P, Paradis V, Ratziu V, et al. Quantification of apolipoprotein A-I and B messenger RNA in heavy drinkers according to liver disease. Hepatology 1996;23:44–51.
Mesejo A, Juan M, Serrano A. Liver cirrhosis and encephalopathy: clinical and metabolic consequences and nutritional support. Nutr Hosp 2008;23(Suppl. 2):8–18.
Myung SJ, Yoon JH, Kim BH, Lee JH, Jung EU, Lee HS. Heat shock protein 90 inhibitor induces apoptosis and attenuates activation of hepatic stellate cells. J Pharmacol Exp Ther 2009.
Parsons CJ, Takashima M, Rippe RA. Molecular mechanisms of hepatic fibrogenesis. J Gastroenterol Hepatol 2007;22(Suppl. 1):S79–84.

Perez MJ, Sanchez-Medina F, Torres M, Gil A, Suarez A. Dietary nucleotides enhance the liver redox state and protein synthesis in cirrhotic rats. J Nutr 2004;134:2504–8.

Priya S, Sudhakaran PR. Curcumin-induced recovery from hepatic injury involves induction of apoptosis of activated hepatic stellate cells. Indian J Biochem Biophys 2008;45:317–25.

Ramadori G, Knittel T, Odenthal M, Schwogler S, Neubauer K, Meyer zum Buschenfelde KH. Synthesis of cellular fibronectin by rat liver fat-storing (Ito) cells: regulation by cytokines. Gastroenterology 1992;103: 1313–21.

Rojkind M, Gonzalez E. An improved method for determining specific radioactivities of proline-14C and hydroxyproline-14C in collagen and in noncollagenous proteins. Anal Biochem 1974;57:1–7.

Stefanovic B, Hellerbrand C, Holcik M, Briendl M, Aliebhaber S, Brenner DA. Post-transcriptional regulation of collagen alpha1(I) mRNA in hepatic stellate cells. Mol Cell Biol 1997;17:5201–9.

Tsukada S, Westwick JK, Ikejima K, Sato N, Rippe RA. SMAD and p38 MAPK signaling pathways independently regulate alpha1(I) collagen gene expression in unstimulated and transforming growth factor-beta-stimulated hepatic stellate cells. J Biol Chem 2005;280:10055–64.

Van Rossen E, Vander Borght S, van Grunsven LA, Reynaert H, Bruggeman V, Blomhoff R, et al. Vinculin and cellular retinol-binding protein-1 are markers for quiescent and activated hepatic stellate cells in formalin-fixed paraffin embedded human liver. Histochem Cell Biol 2009;131:313–25.

Verrecchia F, Mauviel A. Transforming growth factor-beta and fibrosis. World J Gastroenterol 2007;13:3056–62.

Yamamoto H, Sugihara N. Blood ammonia levels and hepatic encephalopathy induced by CCl4 in rats. Toxicol Appl Pharmacol 1987;91:461–8.

Yamamoto HA, Sugihara N. Hepatic ATP content and hyperammonemia induced by CCl4 in rats. Toxicology 1988;51:111–7.

Yang L, Chan CC, Kwon OS, Liu S, McGhee J, Stimpson SA, et al. Regulation of peroxisome proliferator-activated receptor-gamma in liver fibrosis. Am J Physiol Gastrointest Liver Physiol 2006;291:G902–11.

Yassuda Filho P, Bracht A, Ishii-Iwamoto EL, Lousano SH, Bracht L, Kelmer-Bracht AM. The urea cycle in the liver of arthritic rats. Mol Cell Biochem 2003;243:97–106.

Yin MF, Lian LH, Piao DM, Nan JX. Tetrandrine stimulates the apoptosis of hepatic stellate cells and ameliorates development of fibrosis in a thioacetamide rat model. World J Gastroenterol 2007;13:1214–20.

Zannis VI, Kan HY, Kritis A, Zanni E, Kardassis D. Transcriptional regulation of the human apolipoprotein genes. Front Biosci 2001;6:D456–504.